

Nitric oxide blocks hKv1.5 channels by S-nitrosylation and by a cyclic GMP-dependent mechanism

Lucía Núñez^{a,1}, Miguel Vaquero^{a,1}, Ricardo Gómez^a, Ricardo Caballero^{a,*},
Petra Mateos-Cáceres^b, Carlos Macaya^b, Isabel Iriepa^c, Enrique Gálvez^c,
Antonio López-Farré^b, Juan Tamargo^a, Eva Delpón^a

^a Department of Pharmacology, School of Medicine, Universidad Complutense, 28040 Madrid, Spain

^b Cardiovascular Research Unit, Hospital Clínico San Carlos, Madrid, Spain

^c Department of Organic Chemistry, School of Pharmacy, Universidad de Alcalá de Henares, Madrid, Spain

Received 13 March 2006; received in revised form 30 May 2006; accepted 15 June 2006

Available online 27 June 2006

Time for primary review 32 days

Abstract

Objective: This study was undertaken to analyze whether nitric oxide (NO) modulates the human potassium channel hKv1.5, which generates the ultrarapid delayed rectifier current (I_{Kur}) that determines the height and duration of atrial action potentials.

Methods: Currents were recorded using the whole-cell patch-clamp in *Ltk*⁻ cells expressing hKv1.5 channels.

Results: The NO donors (\pm)-S-Nitroso-N-acetylpenicillamine (SNAP) and sodium nitroprusside, a NO solution, and L-Arginine inhibited hKv1.5 currents in a concentration-dependent manner. The NO concentration in the cell chamber was monitored using a sensor, and the IC_{50} for NO-induced hKv1.5 block was 340 ± 70 nM. SNAP also inhibited the I_{Kur} recorded in mouse ventricular myocytes. The NO effects were partially mediated by the activation of the soluble guanylate cyclase (sGC)/cGMP/cGMP-dependent protein kinase (PKG) pathway. The biotin-switch assay demonstrated the presence of S-nitrosylated cysteines (Cys) on the hKv1.5 protein in SNAP-treated cells. Molecular modeling of hKv1.5 channel structure suggests that S-nitrosylation of Cys331 (segment 2, S2) and Cys346 (S2) would be stabilized by hydrogen bridge bonds with Ile262 (S1) and Arg342 (S2), respectively.

Conclusions: NO inhibits the hKv1.5 current by a cGMP-dependent mechanism and by the S-nitrosylation of the hKv1.5 protein, an effect that contributes to shaping the human atrial action potentials.

© 2006 European Society of Cardiology. Published by Elsevier B.V. All rights reserved.

Keywords: Nitric oxide; K-channels; Ion channels; Repolarization; Pharmacology

This article is referred to in the Editorial by I. Baró (pages 7–8) in this issue.

1. Introduction

Nitric oxide (NO) is a diffusible messenger that plays a key role in the cardiovascular system [1]. NO indirectly regulates cardiac function through its modulation of the coronary reserve and peripheral hemodynamics. Further-

more, NO directly regulates many cardiac functions including contraction, relaxation and rate, as well as the mitochondrial respiration, the cellular redox state, and the hypertrophy and apoptosis processes. Indeed, both the excessive and/or defective myocardial production of endogenous NO has been implicated in various pathological states like cardiac failure and postinfarction ventricular remodeling [1–4].

In the human atrial myocardium the action potential (AP) duration and refractoriness are largely determined by the balance between the inward L-type Ca^{2+} current ($I_{Ca,L}$) and several outward K^{+} currents [5,6]. One of these K^{+} currents, the ultrarapid component of the delayed rectifier (I_{Kur}), is

* Corresponding author. Tel.: +34 913941474; fax: +34 913941470.

E-mail address: rcaballero@ift.csic.es (R. Caballero).

¹ These authors contributed equally to this work.

exclusively present in the atria compared to the ventricular tissue and critically determines the duration and the membrane potential level of the plateau phase [5,6]. Previous reports demonstrated that NO inhibits the fast component of the delayed rectifier current (I_{Kr}) [7], whereas it increases the slow component (I_{Ks}) [8]. However, the effects of NO on the I_{Kur} , which is carried by hKv1.5 channels [5,6], are presently unknown. In contrast, the effects of NO-donors on $I_{Ca,L}$ have been extensively studied, and both inhibitory and increasing effects were described. Inhibitory effects were attributed to a redox reaction on thiol groups of the channel, whereas increasing effects were due to the inhibition of the cGMP-induced inhibition of cGMP-inhibited phosphodiesterase [9,10].

In the human atria the maintenance of the duration and the height of the plateau phase determines the excitation–contraction coupling, and is critical for the prevention of the occurrence of the periodic activity of sustained, high frequency, functional reentrant sources (rotors) that can be responsible for the most common arrhythmia, atrial fibrillation (AF) [11]. Therefore, considering the physiological relevance of the modulation of I_{Kur} , we studied the effects of NO on hKv1.5 channels and I_{Kur} , as well as the intracellular signaling pathway responsible for these effects.

2. Methods

2.1. Cell culture, mouse myocyte isolation and solutions

Mouse fibroblasts (Ltk^- cells) stably expressing hKv1.5 channels and untransfected Chinese hamster ovary cells (CHO) were cultured as previously described [12,13], and perfused with an external solution containing (mM): NaCl 130, KCl 4, CaCl₂ 1, MgCl₂ 1, HEPES 10 and glucose 10 (pH 7.4 with NaOH). CD-1 mice ventricular myocytes were enzymatically isolated and perfused with the same external solution supplemented with tetrodotoxin 0.03 mM and CoCl₂ 2 mM as described [12,14]. Recording pipettes were filled with internal solution containing (mM): K-aspartate 80, KCl 42, KH₂PO₄ 10, MgATP 5, phosphocreatine 3, HEPES 5 and EGTA 5 (pH 7.2 with KOH). The investigation conforms with the *Guide for the Care and Use of Laboratory Animals* published by the US National Institutes of Health (NIH Publication No. 85-23, revised 1996).

The NO donors (\pm)-*S*-Nitroso-*N*-acetylpenicillamine (SNAP, Calbiochem, Germany) and sodium nitroprusside (SNP, Sigma, USA) were initially dissolved in ethanol and water, respectively, to yield 0.01 M stock solutions. Control solutions contained the same solvent concentration as the test solution. NO donor solutions were prepared fresh for each experiment. To prepare the NO solution, the external solution was bubbled with argon (Ar) for 20–30 min in a gas wash bottle obtaining an O₂-free solution and, then, with NO (450 ppm NO/Ar) [15]. The NO concentration was monitored in real time in the chamber where the electrophysiological experiments were done, with an ISO-NO meter (World

Precision Instruments Inc., United Kingdom) coupled to a data acquisition hardware and recording software Chart v4.12 (PowerLab, and AD Instruments, Panlab, Spain) [16]. Cells were superfused with NO or NO donor solutions until steady-state effects were reached (\approx 10 min), and thereafter with drug-free solution (washout). Over the mean duration of the experiments the hKv1.5 current in control conditions remained unaffected (see inset in Fig. 2A).

2.2. Recording techniques and analysis

hKv1.5 and I_{Kur} currents were recorded using the whole-cell patch-clamp configuration at \approx 24 °C with 200B patch-clamp amplifiers (Axon Instruments, USA). Capacitance and series resistance were optimized, and \approx 80% compensation was usually obtained. Maximum hKv1.5 current amplitudes at +60 mV averaged 1.5 ± 0.2 nA, and mean uncompensated access resistance and cell capacitance 2.4 ± 0.6 M Ω and 10.8 ± 0.6 pF, respectively ($n=28$). Maximum outward K⁺ current amplitude in mouse ventricular myocytes at +50 mV averaged 2.3 ± 0.4 nA, whereas mean capacitance, access resistance and uncompensated access resistance were 211 ± 34 pF, 5.9 ± 1.6 M Ω , and 1.7 ± 0.4 M Ω , respectively ($n=7$). Thus, under these conditions no significant voltage errors (<5 mV) due to series resistance were expected with the micropipettes used (tip resistance <3.5 M Ω). To obtain the concentration that produces the half-maximum blockade (IC_{50}) and the Hill coefficient (n_H), the fractional block obtained at various drug concentrations was fitted to the Hill equation.

2.3. Detection of NO synthase (NOS), soluble guanylate cyclase (sGC) and S-nitrosylation

NOS1, NOS3, and sGC expression were analyzed in Ltk^- and CHO cells by Western blot using monoclonal IgG antibodies as described [17]. Briefly, proteins were separated in denaturing SDS 10% polyacrylamide gels and blotted onto nitrocellulose. After incubation of the Western blots with the corresponding monoclonal antibodies against NOS1, NOS3 and sGC (Transduction Laboratories, USA), they were detected by chemoluminescence (ECL, Amersham International, United Kingdom). NO production in Ltk^- cells was analyzed by confocal microscopy (Leica, Germany) with the fluorescent indicator 4,5-diaminofluoresceine diacetate (DAF 1 μ M, Sigma) [18].

To determine the putative nitration of hKv1.5 proteins by SNAP, the content of nitrotyrosine protein was measured in control cells and cells treated with 200 μ M SNAP as previously described [19]. Detection of S-nitrosylated hKv1.5 was performed using the biotin-switch assay followed by Western blot as described [20]. Briefly, cells were lysed in a non-denaturing solution (in mM: Tris–HCl 50, NaCl 300, EDTA 5, neocuproine 0.1, and 1% Triton X-100 plus aprotinin and leupeptin). Extracts were adjusted to 0.5 mg/mL and incubated with ethanol for 15 min or 200 μ M SNAP for 5, 15 and 30 min. SNAP was removed by

centrifugation (3500 rpm) with 2 volumes of cold acetone at 4 °C for 10 min. After resuspending the pellet in the non-denaturing lysis solution, extracts were blocked with 4 volumes of blocking buffer (in mM: HEPES 225, EDTA 0.9, neocuproine 0.09, methyl methanethiosulfonate 20 and 2.5% SDS) for 20 min at 50 °C with agitation. Proteins were acetone-precipitated and resuspended in 0.1 mL HENS buffer (mM: HEPES 250, EDTA 1, neocuproine 0.1 and 1% SDS) per mg of protein. Subsequently, extracts were incubated with 1/3 volume of *N*-[6-(biotinamido)hexyl]-3'-(2'-pyridyl-dithio)propionamide (biotin-HPDP, Pierce, USA) and ascorbate 1 mM for 1 h at room temperature. After another acetone precipitation, the pellet was resuspended in 4 μ L HENS buffer. To detect biotinylated proteins by Western blot, samples were incubated with streptavidin–peroxidase for 30 min. A parallel gel was developed to determine the expression of hKv1.5 protein. Since the cysteine (Cys) biotinylation is highly reversible, samples were prepared without reducing agents. To prevent biotin–HPDP nonspecific reactions, samples were not boiled before electrophoresis. All these procedures were carried out in darkness.

2.4. Molecular modeling

Molecular modeling was performed with QUANTA/CHARMm software (Accelrys, France) [13]. The Kv1.2 structure (to date the closest crystallized relative of Kv1.5) was retrieved from Protein Data Bank and used as the template for an hKv1.5 homology model (88% homology). Then, energy minimization was performed to eliminate close contacts. NO was assembled within QUANTA using standard bond lengths and angles. Mechanics energy minimization was done using the CHARMm force field. The NO was manually docked into the Cys thiol. Then, the corresponding complexes were minimized with a Newton Raphson method considering the structures as fully optimized when the energy changes between two successive iterations were less than 0.01 kcal/mol [13].

2.5. Statistical methods

Results are expressed as mean \pm SEM. For each experiment absolute values of current amplitude in control conditions and in the presence of drug were compared by ANOVA followed by Newman–Keuls test. Percentages of block at a single voltage (+60 mV) obtained among different group of experiments were also compared using an ANOVA. A value of $P < 0.05$ was considered significant.

3. Results

3.1. sGC and NOS expression in cell culture

Western blot analysis for comparing the expression level of NOS1, NOS3 and sGC between *Ltk*⁻ and CHO cells demonstrated a higher expression of the three enzymes in

Ltk⁻ than in CHO cells (Fig. 1A). No differences in the loading control (β -actin) were observed. Confocal microscopy experiments confirmed the NO production in *Ltk*⁻ cells incubated with 100 μ M L-Arginine by using the NO specific fluorescent indicator DAF, which reacts covalently with NO to yield the fluorescent triazolofluorescein (Fig. 1B). Therefore, *Ltk*⁻ cells were used as expression system for the analysis of the effects of NO on hKv1.5 channels.

3.2. Effects of NO and NO donors on hKv1.5 currents

Fig. 2A shows hKv1.5 currents recorded by applying 500 ms-pulses from -80 to +60 mV and tail currents upon repolarization to -40 mV in the absence and the presence of 200 μ M SNAP. SNAP reduced the current amplitude at the end of the pulse by 30.7 \pm 5.5% ($n = 6$, $P < 0.05$). These effects were reversible upon washout after 8–12 min with a drug-free solution. SNAP did not modify the time course of current inactivation, measured from the monoexponential fits of the current traces elicited at +60 mV (Table 1). Furthermore, SNAP did not modify the kinetics of tail currents elicited on repolarization to -40 mV after pulses to +60 mV and thus, the fast (τ_f) and the slow (τ_s) time constants of deactivation remained unaltered (Table 1). The concentration dependence of the blockade measured at the end of 500 ms-pulses to +60 mV was fitted to the Hill equation and yielded an IC_{50} of 351 \pm 66 μ M ($n_H = 0.9 \pm 0.1$) (Fig. 2B). A similar IC_{50} was obtained when the n_H was fixed to unity (331 \pm 48 μ M). Fig. 2C shows the electrical signal recorded by the NO sensor during the development of the experiment shown in Fig. 2A. In 6 experiments the NO concentration reached a maximum within 5 min (194 \pm 13 nM) and remained stable during the perfusion with SNAP (\approx 15 min), decreasing to the basal level after 10 min of

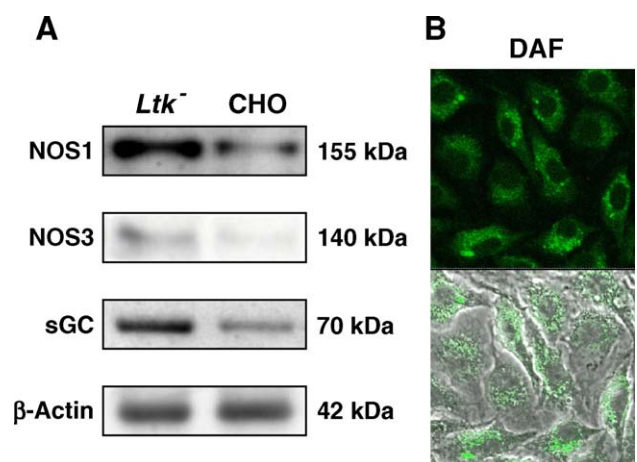


Fig. 1. (A) Representative Western blots demonstrating NOS1, NOS3, sGC, and β -actin expression in *Ltk*⁻ and CHO cells. (B) Fluorescent photomicrograph of confocal microscopic image of *Ltk*⁻ cells showing *in situ* detection of NO with the fluorescent probe DAF (green fluorescence). The upper panel shows the immunofluorescence picture whereas the bottom panel shows the combination of the immunofluorescence picture with the optical microscopy photomicrograph.

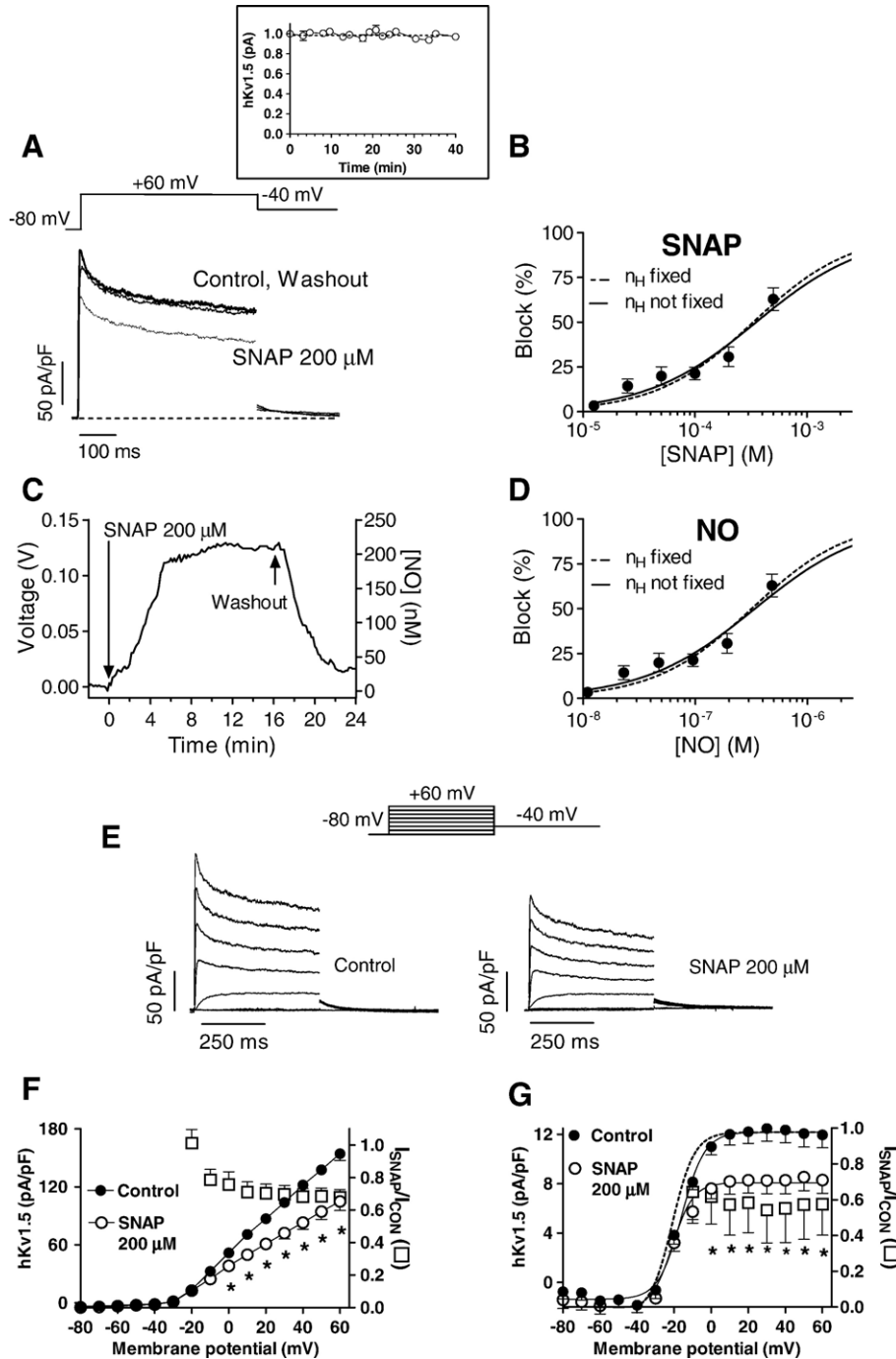


Fig. 2. (A) hKv1.5 currents elicited in *Ltk⁻* cells by 500 ms-pulses from -80 to +60 mV and tail currents recorded upon repolarization to -40 mV in the absence, presence and after washout of 200 μM SNAP. The inset shows the normalized hKv1.5 current amplitude under control conditions over the mean duration of the experiments ($n=16$). (B, D) Concentration dependence of the effects of SNAP as a function of the concentration of SNAP (B) and of the concentration of NO released (D). Dashed and continuous lines represent the fit to the Hill equation fixing the n_H to unity or not, respectively. (C) NO concentrations yielded before and after perfusion of 200 μM SNAP as a function of time. Arrows indicate the beginning and the end of the perfusion with the SNAP solution. (E) hKv1.5 currents elicited with the voltage protocol illustrated at the top in the absence (left) and presence (right) of 200 μM SNAP. (F) Mean current–voltage relationships of hKv1.5 currents in the absence and presence of SNAP. (G) Activation curves in the absence and presence of SNAP. The dashed line represents the fit of the activation curve in the presence of SNAP normalized to the control amplitude. In F and G, squares represent the relative current as a function of the membrane potential. * $P<0.05$ vs. control data. In B, D, F and G, each data point represents the mean \pm SEM of ≥ 5 experiments.

perfusion with SNAP-free solution. Since the NO concentration was monitored in all the experiments, in Fig. 2D the SNAP-induced block was represented as a function of NO

concentration. Fitting the data to the Hill equation yielded an IC_{50} of 340 ± 70 nM ($n_H=0.9 \pm 0.2$) and of 318 ± 46 nM when the n_H was fixed to unity.

Table 1
Effects of NO donors on hKv1.5 currents

		SNAP (200 μ M)	NO solution	SNP (100 μ M)	L-Arginine (10 mM)
$\tau_{\text{inactivation}}$ (ms)	Control	137.8 \pm 37.4	184.2 \pm 5.8	170.1 \pm 30.7	178.2 \pm 23.5
	Drug	124.4 \pm 26.4	176.8 \pm 17.7	184.9 \pm 54.9	178.7 \pm 21.6
$\tau_{\text{fdeactivation}}$ (ms)	Control	26.4 \pm 4.8	31.9 \pm 4.1	21.9 \pm 9.1	30.2 \pm 3.3
	Drug	23.5 \pm 4.5	35.5 \pm 2.5	42.9 \pm 6.2	43.2 \pm 7.1
$\tau_{\text{sdeactivation}}$ (ms)	Control	111.4 \pm 21.9	119.5 \pm 14.1	171.1 \pm 11.1	176.0 \pm 54.4
	Drug	123.6 \pm 21.8	115.9 \pm 13.1	131.8 \pm 37.6	166.6 \pm 34.9
$A_{\text{s}}/A_{\text{f}}$	Control	0.65 \pm 0.1	0.61 \pm 0.1	0.65 \pm 0.1	0.73 \pm 0.2
	Drug	0.72 \pm 0.1	0.72 \pm 0.2	0.65 \pm 0.1	0.70 \pm 0.1
$V_{\text{hactivation}}$ (mV)	Control	-14.6 \pm 3.4	-16.5 \pm 0.6	-16.6 \pm 1.1	-15.2 \pm 1.6
	Drug	-19.7 \pm 3.9*	-22.9 \pm 1.5*	-22.1 \pm 1.1*	-21.2 \pm 1.6*
$k_{\text{activation}}$ (mV)	Control	4.1 \pm 0.7	4.9 \pm 0.5	4.3 \pm 0.9	4.8 \pm 0.3
	Drug	4.0 \pm 0.7	4.8 \pm 0.7	4.0 \pm 0.9	4.3 \pm 1.1

Data are mean \pm SEM of >6 experiments. * P <0.05 vs. control.

Families of current traces recorded by applying the pulse protocol at the top for control conditions and after 200 μ M SNAP exposure are shown in Fig. 2E. Current voltage plots of current amplitude measured at the end of the depolarizing pulse (current–voltage relationship) and peak tail current (activation curve) are depicted in Fig. 2F and G, respectively. In both panels, squares represent the relative current. The blockade of the current amplitude at the end of the pulse was apparent at -10 mV (21.4 \pm 6.4%) and thereafter it progressively increased at more depolarized potentials ($n=6$, P <0.05 vs. block at +60 mV). SNAP also decreased the tail current amplitude at potentials positive to 0 mV (42.4 \pm 17.2% at +60 mV, $n=5$, P <0.05). Activation curves were fitted to a Boltzmann equation (continuous lines). SNAP shifted the midpoint of activation curve (V_{h}) toward more negative potentials without modifying the slope (k) values (Table 1 and Fig. 2G).

To confirm that the SNAP effects were exclusively attributable to the released NO, we next studied the effects of a NO solution (see Methods) and another NO donor, SNP. Fig. 3A shows the NO concentrations monitored during perfusion with the NO solution in the experiment shown in Fig. 3B. The NO concentration reached a steady state within \approx 10 min (216 \pm 8 nM, $n=6$) and remained stable during the perfusion. NO solution and 100 μ M SNP decreased the current amplitude at +60 mV by 33.9 \pm 9.8% ($n=6$, Fig. 3B), and 25.0 \pm 5.5% ($n=5$, Fig. 3C), respectively, effects that were reversible upon washout. As observed in the presence of SNAP, NO solution and SNP modified the voltage dependence of the activation, whereas they did not modify either the deactivation or the inactivation kinetics (Table 1). Fig. 3D represents the concentration dependence of the SNAP-induced block, and the inset the NO concentration released in the presence of SNAP. The blockade measured at the end of 500 ms-pulses to +60 mV was fitted to the Hill equation, yielding an IC_{50} value of 19.8 \pm 4.2 μ M ($n_{\text{H}}=1.6\pm 0.3$) with a maximum blockade (B_{max}) of 22.0 \pm 6.3%. When the n_{H} was fixed to

unity, the IC_{50} and the B_{max} averaged 15.7 \pm 6.1 μ M and 23.1 \pm 15.4%, respectively.

Finally, the effects of the endogenous NO precursor, L-Arginine, were studied. Fig. 3E shows current traces recorded by applying 500 ms-pulses from -80 to +60 mV, in the absence and presence of 10 mM L-Arginine. L-Arginine reduced the current amplitude by 24.3 \pm 3.8% ($n=6$, P <0.05) without modifying either the inactivation or the deactivation time course. In contrast, L-Arginine shifted the V_{h} toward hyperpolarized potentials (Table 1). Fig. 3F shows the effects of L-Arginine in the presence of 10 mM N^{G} -Nitro-L-Arginine methyl ester (L-NAME, Sigma), which inhibits the NOS [21]. L-NAME alone did not modify hKv1.5 currents, and, in the presence of L-NAME, L-Arginine did not decrease the hKv1.5 current ($n=6$, P >0.05).

3.3. Effects of NO on I_{Kur} recorded in mouse myocytes

We next studied the effects of SNAP on I_{Kur} recorded in mouse ventricular myocytes. A 200 ms-prepulse to +40 mV was applied to inactivate I_{to} [12,14], followed by a 500 ms-pulse to +50 mV (Fig. 4A), eliciting a slowly inactivating delayed rectifier outward K^+ current. This current is composed of at least two components: I_{Kslow1} and I_{Kslow2} , generated by Kv1.5 and Kv2.1 channels, respectively, where only the component carried by Kv1.5 channels exhibits slow inactivation [12,14]. SNAP inhibited the current (measured as the difference between the peak current and the current at the end of the pulse) elicited by the pulse to +50 mV by 50.1 \pm 3.0% ($n=7$) (Fig. 4B), without modifying the time course of current decay ($\tau_{\text{C}}=328.1\pm 80.9$ ms vs. $\tau_{\text{SNAP}}=310.2\pm 58.9$ ms, $n=7$, P >0.05).

3.4. Signaling pathway involved in the effects of NO on hKv1.5 currents

The sGC/cGMP/cGMP-dependent protein kinase (PKG) signaling pathway is the most common mechanism

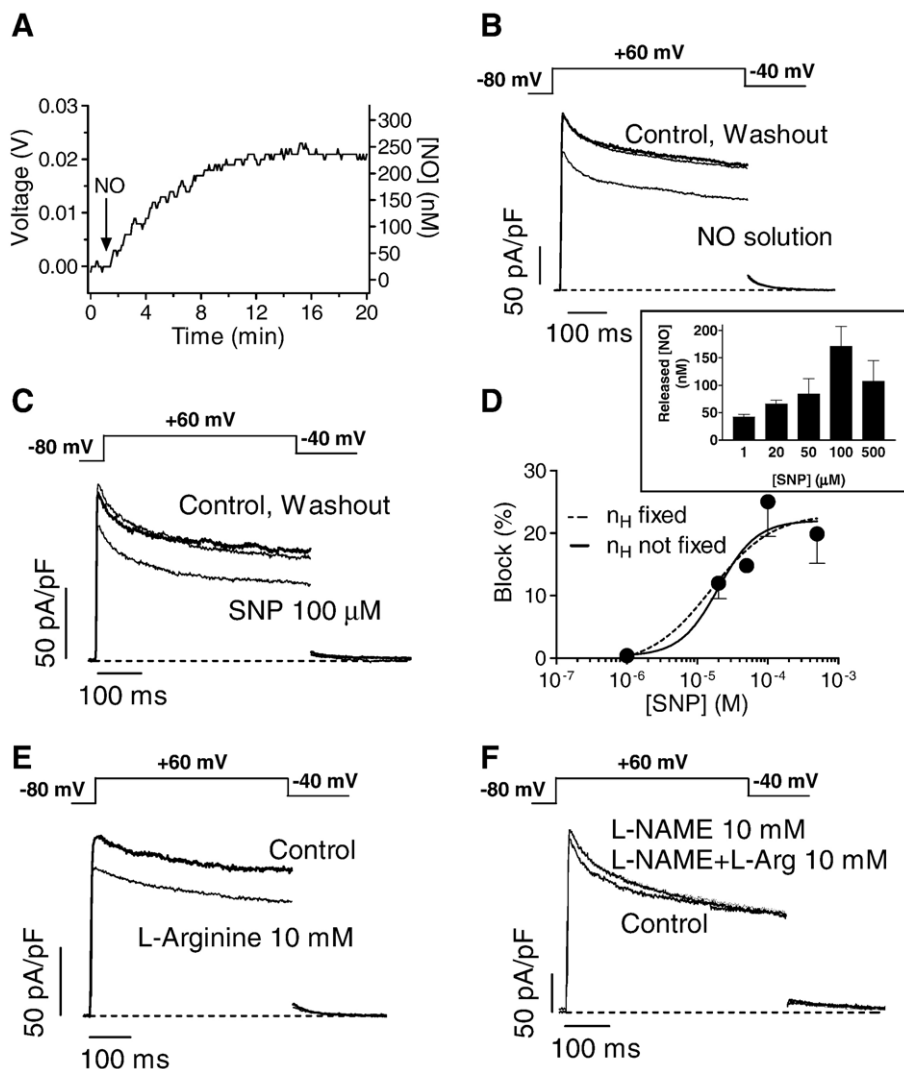


Fig. 3. (A) NO concentrations yielded before and after perfusion of the NO solution. The arrow indicates the beginning of the perfusion with the NO solution. hKv1.5 currents elicited in *Ltk⁻* cells by pulses from -80 to $+60$ mV in the absence and presence of NO solution (B) and SNP (C). (D) Concentration–response curve of SNP. Dashed and continuous lines represent the fit to the Hill equation fixing the n_H to unity or not, respectively. Each data point represents the mean \pm SEM of 6 experiments. The inset shows the NO concentration released at each SNP concentration. (E) hKv1.5 currents elicited by pulses from -80 to $+60$ mV in the absence and presence of 10 mM L-Arginine. (F) Current traces in control conditions and in the presence of 10 mM L-NAME alone or plus L-Arginine.

implicated in NO effects. For testing whether this pathway was responsible for the effects, we first studied the effects of SNAP in the presence of 1H-[1,2,4]Oxadiazolo[4,3-a]quinoxalin-1-one (ODQ, Sigma), a selective inhibitor of sGC. ODQ (50 μ M) alone inhibited hKv1.5 current at the end of the 500 ms-pulses to $+60$ mV by $15.4 \pm 4.9\%$, and the addition of 200 μ M SNAP further decreased the current by $17.7 \pm 5.8\%$ ($n=6$), contrasting with the $30.7 \pm 5.5\%$ produced by SNAP alone ($P < 0.05$, Fig. 5A). Second, we examined the effects of SNAP in the presence of KT5823 (Calbiochem), a PKG inhibitor. In the presence of 1 μ M KT5823 (which inhibited the current by $3.5 \pm 0.1\%$, $n=6$), SNAP decreased the current elicited by pulses to $+60$ mV only by $16.8 \pm 4.0\%$, a blockade significantly lower than that produced by SNAP alone ($P < 0.05$, Fig. 5B). Finally, the effect of 500 μ M 8-bromo-cGMP (8Br-cGMP, Calbiochem),

a potent cell-permeable PKG activator, on hKv1.5 currents was studied. 8Br-cGMP mimicked only part of the blockade produced by SNAP ($18.3 \pm 0.6\%$, $n=6$) (Fig. 5C). All these results demonstrated that the effects produced by SNAP were partially mediated by the activation of the sGC/cGMP/PKG pathway.

3.5. Post-translational modifications of hKv1.5 protein by NO

NO can regulate protein functions by post-translational modifications including Cys S-nitrosylation and tyrosine (Tyr) nitration [22]. Since S-nitrosylation and nitration are highly dependent on the cellular redox state, we first studied the effects of SNAP in the presence of the thiol-specific reducing agent, dithiothreitol (DTT, Sigma). Fig. 5D shows

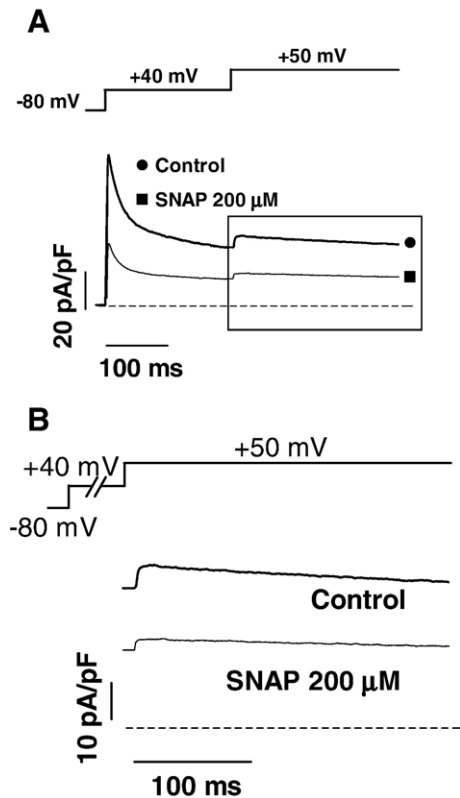


Fig. 4. (A) Outward K^+ currents elicited in mouse myocytes by applying a 200 ms-prepulse to +40 mV followed by a test pulse to +50 mV. (B) K^+ currents obtained with the pulse to +50 mV in the absence and presence of 200 μ M SNAP.

that 5 mM DTT inhibited the current at the end of 500 ms-pulse to +60 mV by $29.6 \pm 1.6\%$ ($P < 0.05$). The addition of SNAP in the presence of DTT, further inhibited the current by $23.3 \pm 1.8\%$ ($n = 6$, $P < 0.05$), a blockade that was lower than that produced by SNAP alone ($P < 0.05$). These results suggested the implication of post-translational modifications in the effects of SNAP in hKv1.5 currents.

The putative hKv1.5 Tyr nitration was measured by the immunoprecipitation of hKv1.5 protein followed by Western blot using an anti-nitrotyrosine antibody. Treatment with SNAP did not promote the nitration of hKv1.5 protein (data not shown), indicating that this mechanism was not responsible for its effects. Thus, we tested whether S-nitrosylation was involved. For this purpose, the putative hKv1.5 S-nitrosylated protein was labelled with biotin using biotin-HPDP and detected with streptavidin-peroxidase following the biotin-switch assay [20]. Representative Western blot (Fig. 5E top) obtained after the assay demonstrated the presence of S-nitrosylated Cys residues on the hKv1.5 protein only in SNAP treated cells. However, all the samples showed a similar expression of hKv1.5 protein (Fig. 5E middle). Equal loading of the blots was confirmed by a parallel Western blot performed with β -actin antibody (Fig. 5E bottom). Quantification revealed that the S-nitrosylation reached a maximum in cells treated with

SNAP for 15 min, coinciding with the time at which current recordings were performed (Fig. 5F).

4. Discussion

Our results demonstrate for the first time that NO, its precursor L-Arginine, and the NO donors, SNAP and SNP, block human cardiac Kv1.5 channels expressed in *Ltk*⁻ cells. Moreover, SNAP inhibited native I_{Kur} in mouse ventricular myocytes, which exhibit a robust current generated by Kv1.5 channels [12,14]. The data also demonstrated that the NO effects are the consequence of both the activation of sGC/cGMP/PKG pathway and the S-nitrosylation of Cys residues.

4.1. NO inhibition of hKv1.5 and I_{Kur} currents

NO produced a concentration-dependent inhibition of hKv1.5 currents, the IC_{50} being around 350 nM. It is worth noting that the inhibitory effects of hKv1.5 channels exhibited the same voltage- and time-dependence independently of whether the NO was released or not by SNAP. Furthermore, it should be stressed that SNAP also blocked the native I_{Kur} demonstrating that the results obtained in cloned hKv1.5 channels expressed in mouse fibroblasts are reproduced in native cardiac cells.

However, in our experimental conditions, blockade produced by SNP was significantly lower than that produced by SNAP or NO. This can be explained because under our experimental conditions (in darkness and with a limited number of isolated cells in the patch chamber) SNP is not an efficient NO donor, since it has been proposed that NO liberation by SNP requires either light irradiation or one-electron reduction mechanism which in biological systems can be both non-enzymatic and enzymatic [23]. In fact, NO concentrations released by SNP did not further increase at SNP concentrations higher than 100 μ M.

We demonstrated that *Ltk*⁻ cells endogenously express NOS1 and NOS3 that were able to synthesize NO from L-Arginine. Furthermore, our results also demonstrated that L-Arginine inhibited the hKv1.5 current, and that this inhibition was abolished by the treatment with L-NAME, a NOS inhibitor.

It should be stressed that NO did not modify the time-dependent properties of hKv1.5 channels (activation, inactivation, and deactivation kinetics). Therefore, NO seems to simply scale down the hKv1.5 current amplitude. This effect is similar to that produced by NO on the inward Na^+ current (I_{Na}) measured in mouse ventricular myocytes [15]. In that study, single channel recordings demonstrated that NO diminished the macroscopic current by decreasing the open probability and/or the number of functional channels rather than by changing their permeation or gating. However, NO modified the voltage dependence of hKv1.5 channels activation by shifting the activation curve toward more negative potentials. Similarly, the NO donors

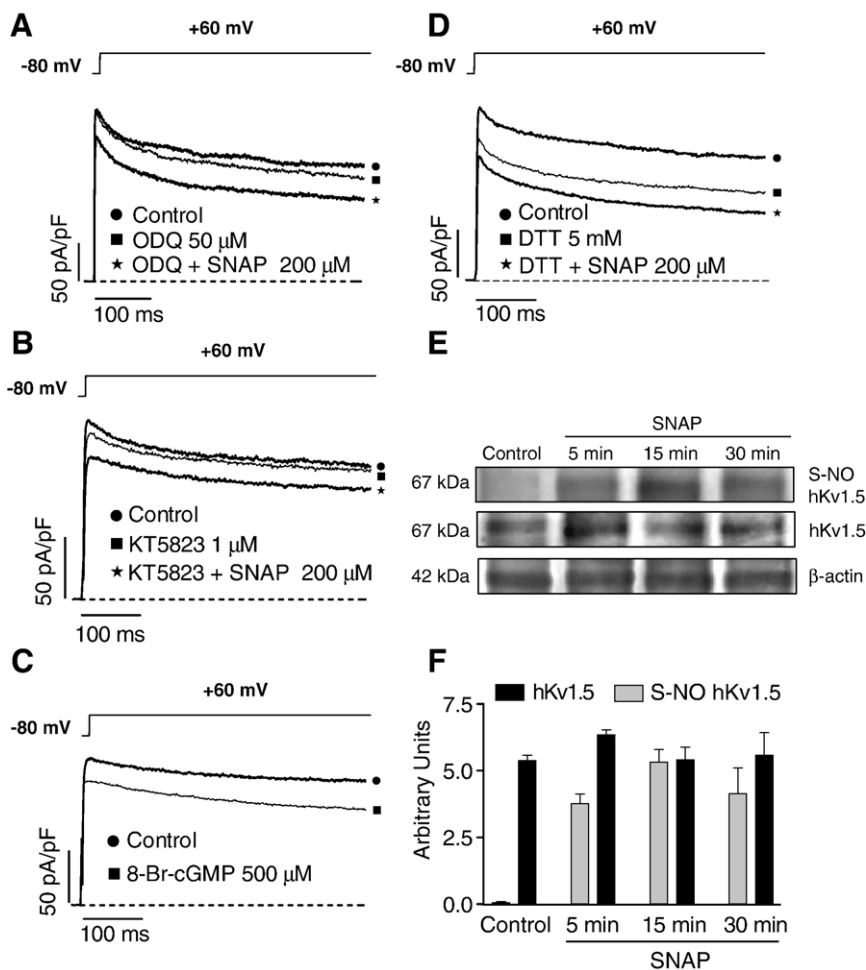


Fig. 5. (A) hKv1.5 currents recorded in *Ltk*⁻ cells by applying pulses from -80 to $+60$ mV in control conditions and in the presence of $50 \mu\text{M}$ ODQ alone and plus $200 \mu\text{M}$ SNAP. (B) Current traces in control conditions and in the presence of $1 \mu\text{M}$ KT5823 alone and plus $200 \mu\text{M}$ SNAP. (C) Current traces in the absence and presence of $500 \mu\text{M}$ 8-Br-cGMP. (D) hKv1.5 currents in control conditions and in the presence of 5 mM DTT alone and plus $200 \mu\text{M}$ SNAP. (E) Representative Western blots showing S-nitrosylated hKv1.5 (top), hKv1.5 (middle) and β -actin (bottom) expression, in control conditions or in cells incubated with $200 \mu\text{M}$ SNAP at different times (5, 15 and 30 min). (F) Bar graph showing the densitometric scanning of the Western blots. Results are presented as mean \pm SEM of >5 experiments.

decreased Kv11.1 (HERG) currents by shifting the voltage-dependence of the inactivation process toward more negative potentials [7].

4.2. Signaling pathway involved in the effects of NO on hKv1.5 currents

NO can exert many of its effects through an indirect pathway involving activation of sGC and increased levels of cGMP. The NO-induced block was partially reproduced by the application of 8Br-cGMP, a cell-permeable analogue of cGMP, and can also be partially suppressed in the presence of sGC and PKG inhibitors. These results suggest that the inhibitory effects of NO are partially dependent on the sGC/cGMP/PKG pathway. This signaling pathway has also been implicated in the effects of NO on cardiac I_{Na} [15], $I_{\text{Ca,L}}$ [10], ATP-sensitive K^+ channels (I_{KATP}) [24], and the hyperpolarization-activated inward current, I_f [25].

Our results also demonstrated that the inhibitory effects of NO were partially mediated by a cGMP-independent mechanism, which in turn, depended on the redox state of the cell, since they were decreased in the presence of the reducing agent DTT. It is known that the post-translational effects produced by the incorporation of NO moieties by covalent bonding to proteins depend on the redox state and that these redox-related NO signals are critical for cellular control mechanisms [22,26]. Among them, S-nitrosylation of Cys residues can be considered the most important because of its high reactivity, occurrence in physiological conditions and its influence on many protein functions [22,26]. Previous reaction of NO with O_2 is considered to be necessary for S-nitrosylation, via formation of higher nitrogen oxides, particularly N_2O_3 , which is thought to be the most important S-nitrosylating species [22,26]. Here we found, using the biotin-switch assay, that S-nitrosylation is partially responsible for the effects of NO on hKv1.5

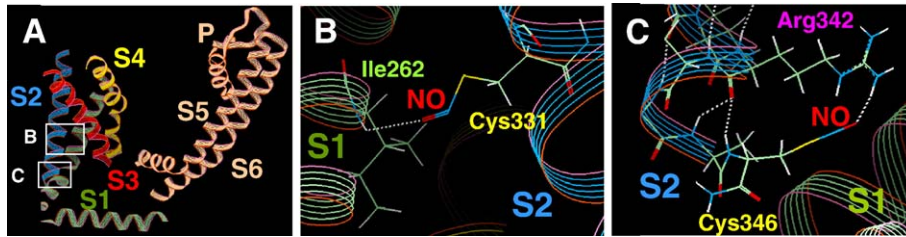


Fig. 6. (A) Molecular modeling of an α -subunit of hKv1.5 channel with the extracellular solution above and the intracellular solution below. (B) Structural detail of S-nitrosylated Cys331 (S2) and the hydrogen bridge bond formed with Ile262 (S1) viewed from the rear. (C) Structural detail of S-nitrosylated Cys346 (S2) and the hydrogen bridge bond formed with Arg342 (S2). P, pore region; S, segment.

channels. In contrast, Tyr nitration, which implies the incorporation of a NO_2 group, is not involved in these effects. Previous studies demonstrated that the S-nitrosylation controls the gating of the ryanodine and the neuronal NMDA receptor associated channels [22]. Furthermore, it has been proposed that redox-related NO post-translational modifications could be responsible for the effects observed on cardiac I_{Ks} [8], I_{Kr} [7], and $I_{Ca,L}$ [10] currents, even when direct evidence of the S-nitrosylation and/or nitration was not provided.

4.3. Molecular modeling of the structure of hKv1.5 channels

Analysis of S-nitrosylation in several proteins demonstrated that formation of nitrosothiols can be favoured in more ionisable Cys, such as those in which the thiolate anion can be stabilized by acid–base interactions with neighbouring groups, belonging to adjacent residues in the primary sequence or just in the proximity in the three-dimensional structure [27]. In fact, a “consensus motif” frequently appeared in those proteins that are S-nitrosylated preceding and following the Cys residue. This sequence pattern was not present in the hKv1.5 channel protein. Therefore, we decided to construct a three-dimensional model of the protein using a homology model approach and the recently crystallized Kv1.2 channel structure as template [28] (Fig. 6A). Molecular modeling revealed that none of the thiol group of the eleven hKv1.5 Cys is located in the vicinity (≈ 6 Å) of an acid and a basic residue that could act as catalysts for nitrosylation. It is accepted that S-nitrosylation is a very labile covalent modification with half-lives ranging from seconds to a few minutes. However, the model suggested that the nitrosothiol groups of two Cys located at the S2 (331 and 346) would be particularly stable because of the formation of hydrogen bridge bonds with residues located in the S1 (Ile262, Fig. 6B) and the S2 (Arg342, Fig. 6C), respectively. Thus, we proposed that the S-nitrosylation of these Cys could be partially responsible for the inhibitory effects produced by NO on hKv1.5 channels. Moreover, since both Cys are located in the hKv1.5 voltage sensor region (S1–S4) [29], their chemical modification could account for the alteration of the voltage-dependence of activation induced by NO.

4.4. Physiological implications

Here we describe that NO blocks hKv1.5 channels, the IC_{50} being around 350 nM. Nanosensing techniques recently described cyclic fluctuations of the NO concentration in the myocardium varying in the range of 200–800 nM [30]. This would imply that, under physiological conditions, NO maintains a “tonic” inhibition of the K^+ efflux through hKv1.5 channels, which in turn would be important for the control of the duration and height of the plateau phase of the human atrial AP. Recently, using a porcine model of AF, it has been demonstrated that AF is associated with a marked decrease in NOS expression and NO bioavailability in atrial tissue [31]. Therefore, it could be hypothesized that under AF conditions the decrease in NO would shorten the duration of the plateau phase by increasing the hKv1.5 current amplitude, an effect that can contribute to the alteration of the atrial electrical properties that lead to the maintenance and recurrence of the arrhythmia (electrical remodeling) [32]. It should be stressed, however, that the plateau duration is the balance among depolarizing (Na^+ and Ca^{2+}) and several repolarizing K^+ currents. Thus, the effects of NO on the other currents have to be studied to accurately predict the resultant effects on the shape of the atrial AP. In conclusion, here we demonstrated that NO inhibits I_{Kur} flowing through hKv1.5 channels by a cGMP-dependent mechanism and by the direct S-nitrosylation of the protein, an effect that could contribute to shape the human atrial AP under physiological conditions.

Acknowledgments

We thank Dr. Pérez-Vizcaíno and Dr. Cogolludo for their helpful suggestions, and Guadalupe Pablo for her excellent technical assistance. Ricardo Gómez is a fellow of the Comunidad Autónoma de Madrid. This work was supported by SAF2005-04609, Mutua Madrileña Foundation, and Red HERACLES (G03/045) Grants.

References

- [1] Schulz R, Rassaf T, Massion PB, Kelm M, Balligand JL. Recent advances in the understanding of the role of nitric oxide in cardiovascular homeostasis. *Pharmacol Ther* 2005;108:225–56.

- [2] Hare JM. Nitric oxide and excitation–contraction coupling. *J Mol Cell Cardiol* 2003;35:719–29.
- [3] Moncada S, Erusalimsky JD. Does nitric oxide modulate mitochondrial energy generation and apoptosis? *Nat Rev Mol Cell Biol* 2002;3:214–20.
- [4] Dawson D, Lygate CA, Zhang MH, Hulbert K, Neubauer S, Casadei B. nNOS gene deletion exacerbates pathological left ventricular remodeling and functional deterioration after myocardial infarction. *Circulation* 2005;112:3729–37.
- [5] Tamargo J, Caballero R, Gómez R, Valenzuela C, Delpón E. Pharmacology of cardiac potassium channels. *Cardiovasc Res* 2004;62:9–33.
- [6] Nerbonne JM, Kass RS. Molecular physiology of cardiac repolarization. *Physiol Rev* 2005;85:1205–53.
- [7] Taglialatela M, Pannaccione A, Tossa S, Castaldo P, Annunziato L. Modulation of the K⁺ channels encoded by the human ether-a-gogo-related gene-1 (hERG1) by nitric oxide. *Mol Pharmacol* 1999;56:1298–308.
- [8] Bai CX, Takahashi K, Masumiya H, Sawanobori T, Furukawa T. Nitric oxide-dependent modulation of the delayed rectifier K⁺ current and the L-type Ca²⁺ current by ginsenoside Re, an ingredient of Panax ginseng, in guinea-pig cardiomyocytes. *Br J Pharmacol* 2004;142:567–75.
- [9] Hu H, Chiamvimonvat N, Yamagishi T, Marbán E. Direct inhibition of expressed cardiac L-type Ca²⁺ channels by S-nitrosothiol nitric oxide donors. *Circ Res* 1997;81:742–52.
- [10] Campbell DL, Stamler JS, Strauss HC. Redox modulation of L-type calcium channels in ferret ventricular myocytes. Dual mechanism regulation by nitric oxide and S-nitrosothiols. *J Gen Physiol* 1996;108:277–93.
- [11] Pandit SV, Berenfeld O, Anumonwo JM, Zaritski RM, Kneller J, Nattel S, et al. Ionic determinants of functional reentry in a 2-D model of human atrial cells during simulated chronic atrial fibrillation. *Biophys J* 2005;88:3806–21.
- [12] Gómez R, Núñez L, Caballero R, Vaquero M, Tamargo J, Delpón E. Spironolactone and its main metabolite canrenoic acid, block hKv1.5, Kv4.3 and Kv7.1+minK channels. *Br J Pharmacol* 2005;146:146–61.
- [13] Moreno I, Caballero R, González T, Arias C, Valenzuela C, Iriepa I, et al. Effects of irbesartan on cloned potassium channels involved in human cardiac repolarization. *J Pharmacol Exp Ther* 2003;304:862–73.
- [14] Brouillette J, Clark RB, Giles WR, Fiset C. Functional properties of K⁺ currents in adult mouse ventricular myocytes. *J Physiol* 2004;559:777–98.
- [15] Ahmmed GU, Xu Y, Hong Dong P, Zhang Z, Eiserich J, Chiamvimonvat N. Nitric oxide modulates cardiac Na⁺ channel via protein kinase A and protein kinase G. *Circ Res* 2001;89:1005–13.
- [16] López-López G, Moreno L, Cogolludo A, Galisteo M, Ibarra M, Duarte J, et al. Nitric oxide (NO) scavenging and NO protecting effects of quercetin and their biological significance in vascular smooth muscle. *Mol Pharmacol* 2004;65:851–9.
- [17] Molero L, López-Farré A, Mateos-Cáceres PJ, Fernández-Sánchez R, Maestro ML, Silva J, et al. Effect of clopidogrel on the expression of inflammatory markers in rabbit ischemic coronary artery. *Br J Pharmacol* 2005;146:419–24.
- [18] Pritchard Jr KA, Ackerman AW, Gross ER, Stepp DW, Shi Y, Fontana JT, et al. Heat shock protein 90 mediates the balance of nitric oxide and superoxide anion from endothelial nitric-oxide synthase. *J Biol Chem* 2001;276:17621–4.
- [19] Sánchez de Miguel L, Arriero MM, Farré J, Jiménez P, García-Méndez A, de Frutos T, et al. Nitric oxide production by neutrophils obtained from patients during acute coronary syndromes: expression of the nitric oxide synthase isoforms. *J Am Coll Cardiol* 2002;39:818–25.
- [20] Jaffrey SR, Erdjument-Bromage H, Ferris CD, Tempst P, Snyder SH. Protein S-nitrosylation: a physiological signal for neuronal nitric oxide. *Nat Cell Biol* 2001;3:193–7.
- [21] Furfine ES, Harmon MF, Paith JE, Garvey EP. Selective inhibition of constitutive nitric oxide synthase by L-NG-nitroarginine. *Biochemistry* 1993;32:8512–7.
- [22] Martínez-Ruiz A, Lamas S. S-nitrosylation: a potential new paradigm in signal transduction. *Cardiovasc Res* 2004;62:43–52.
- [23] Feelisch M. The use of nitric oxide donors in pharmacological studies. *Naunyn Schmiedebergs Arch Pharmacol* 1998;358:113–22.
- [24] Han J, Kim N, Joo H, Kim E, Earm YE. ATP-sensitive K⁺ channel activation by nitric oxide and protein kinase G in rabbit ventricular myocytes. *Am J Physiol* 2002;283:H1545–54.
- [25] Musialek P, Lei M, Brown HF, Paterson DJ, Casadei B. Nitric oxide can increase heart rate by stimulating the hyperpolarization-activated inward current, I(f). *Circ Res* 1997;81:60–8.
- [26] Hess DT, Matsumoto A, Kim SO, Marshall HE, Stamler JS. Protein S-nitrosylation: purview and parameters. *Nat Rev Mol Cell Biol* 2005;6:150–66.
- [27] Stamler JS, Toone EJ, Lipton SA, Sucher NJ. (S)NO signals: translocation, regulation, and a consensus motif. *Neuron* 1997;18:691–6.
- [28] Long SB, Campbell EB, Mackinnon R. Crystal structure of a mammalian voltage-dependent Shaker family K⁺ channel. *Science* 2005;309:897–903.
- [29] Long SB, Campbell EB, Mackinnon R. Voltage sensor of Kv1.2: structural basis of electromechanical coupling. *Science* 2005;309:903–8.
- [30] Malinski T. Understanding nitric oxide physiology in the heart: a nanomedical approach. *Am J Cardiol* 2005;96:13i–24i.
- [31] Cai H, Li Z, Goette A, Mera F, Honeycutt C, Feterik K, et al. Downregulation of endocardial nitric oxide synthase expression and nitric oxide production in atrial fibrillation: potential mechanisms for atrial thrombosis and stroke. *Circulation* 2002;106:2854–8.
- [32] Nattel S. New ideas about atrial fibrillation 50 years on. *Nature* 2002;415:219–26.